Extreme N_2O accumulation in the coastal oxygen minimum zone off Peru

Annette Kock[1], Damian L. Arévalo-Martínez[1], Carolin R. Löscher[2], Hermann W. Bange[1]

[1]GEOMAR Helmholtz Centre for Ocean Research Kiel, Duesternbrooker Weg 20, 24105 Kiel, Germany

[2] Institute of General Microbiology, Christian-Albrechts University Kiel, Am Botanischen Garten 1-9, 24118 Kiel, Germany

Correspondence to: Annette Kock, akock@geomar.de

Abstract

Depth profiles of nitrous oxide (N_2O) were measured during six cruises to the upwelling area and oxygen minimum zone (OMZ) off Peru in 2009 and 2012/2013, covering both the coastal shelf region and the adjacent open ocean. N_2O profiles displayed a strong sensitivity towards oxygen concentrations. Open ocean profiles showed a transition from a broad maximum to a double-peak structure towards the centre of the OMZ where the oxygen minimum was more pronounced. Maximum N_2O concentrations in the open ocean were about 80 nM. A linear relationship between ΔN_2O and apparent oxygen utilization (AOU) could be found for all measurements within the upper oxycline, with a slope similar to studies in other oceanic regions. N_2O profiles close to the shelf revealed a much higher variability, with N_2O concentrations in the upper oxycline reaching up to several hundred nanomoles per liter at selected stations. Due to the extremely sharp oxygen gradients at the shelf, these maxima occurred in very shallow water depths of less than 50 m. In the coastal area, a linear relationship between ΔN_2O and AOU could not be observed as extremely high ΔN_2O values were scattered over the full range of oxygen concentrations. Our results indicate that the coastal upwelling off Peru at the shelf causes conditions that lead to extreme N_2O accumulation, most likely due to the interplay of high rates of nitrogen cycling and a rapid switching of the OMZ waters from anoxic to oxic conditions as a result from coastal upwelling and subsequent strong remineralization in the water column along the Peruvian coast.

1 Introduction

Nitrous oxide (N_2O) acts as a strong atmospheric greenhouse gas and contributes substantially to the stratospheric ozone depletion (IPCC, 2013;WMO, 2011). The ocean is a major source for N_2O as it is naturally produced in the water column (Ciais et al., 2013;Bange, 2008). While in large parts of the surface ocean N_2O concentrations are close to saturation, high emissions of N_2O have been observed in upwelling areas where subsurface waters enriched in N_2O are transported to the surface (e.g. Nevison et al. (2004)). The global distribution of N_2O in the ocean is closely linked to the oceanic oxygen distribution, and particularly high supersaturations are found in upwelling areas which overlay pronounced oxygen minimum zones (OMZ), e.g. in the Arabian Sea (Bange, 2004) or in the eastern South Pacific Ocean (Charpentier et al., 2010).

These OMZs are key regions for the marine nitrogen (N) cycling where active N loss via canonical denitrification and anaerobic ammonium oxidation (anammox) takes place. Recent studies furthermore indicate that they are also zones of intense nitrogen fixation (Deutsch et al., 2007;Loescher et al., 2014;Fernandez et al., 2011), and in areas where the OMZ is fuelled by high export production, high rates of other N transformation processes, such as nitrification, have been observed (Hu et al., 2015;Kalvelage et al., 2013).

Within the nitrogen cycle, N_2O evolves during nitrification and denitrification (Bange, 2008). Both processes strongly depend on the oxygen availability in the water column, with different responses to the oxygen concentration. Under oxic conditions the first step of nitrification, ammonium-oxidation to nitrite, is known to be the main production pathway for N_2O, with an increasing N_2O yield at decreasing oxygen concentrations (Goreau et al., 1980;Löscher et al., 2012;Frame and Casciotti, 2010). During bacterial ammonium-oxidation, N_2O can either be produced as a side product during the oxidation of ammonia to nitrite or through the reduction of nitrite to N_2O (nitrifier-denitrification) (Stein, 2011). Nitrifier-denitrification has been identified as an important production pathway of N_2O at low oxygen concentrations and may thus be responsible for the increased N_2O production under these conditions (Ni et al., 2014).

While the N_2O production pathways during bacterial nitrification have been studied for several decades, archaeal ammonium oxidation has only recently come into focus as a main production pathway for N_2O. The exact mechanism and the extent to which ammonium oxidation or a nitrifier-denitrification pathway are responsible for archaeal N_2O production as well as the effect of environmental controls on archaeal N_2O production are subject to ongoing research (Stieglmeier et al., 2014;Löscher et al., 2012;Santoro et al., 2011).

During denitrification, the canonical reduction of nitrate to molecular nitrogen, N_2O evolves as an intermediate product. Denitrifying genes are widespread among different groups of microorganisms, but active denitrification is restricted to suboxic to anoxic conditions (e.g. Firestone et al., (1980); Dalsgaard et al. (2014)). Denitrification is a heterotrophic process that is stimulated by the supply of organic carbon or hydrogen sulfide (Chang et al., 2014;Dalsgaard et al., 2014;Galan et al., 2014).Depending on the environmental conditions, N_2O production or consumption due to denitrification can be observed in environmental samples. There has been evidence that N_2O consumption is more sensitive to trace amounts of oxygen than N_2O production. This could lead to N_2O accumulation when oxygen is present in low concentrations (Tiedje, 1988). Exceptionally high N_2O concentrations have been measured off the West Indian Coast where anoxic waters from the Arabian Sea frequently extend over the shelf (Naqvi et al., 2000). These are the highest marine N_2O concentrations reported so far and were associated with an increased N_2O production from denitrification during transient oxygen concentrations. In a recent study it was furthermore shown that N_2O production from denitrification could be stimulated by H_2S addition (Dalsgaard et al., 2014) which could indicate a coupling between N_2O production and sulfur cycling.

Measurements of denitrification and anammox rates in different oceanic OMZs have raised the question whether denitrification or anammox is the main pathway for nitrogen loss in the water column (Hamersley et al., 2007;Ward et al., 2009;Voss and Montoya, 2009). In the ETSP, anammox has been found to play the major role in N loss, whereas denitrification was only rarely detectable (Kalvelage et al., 2013;Hamersley et al., 2007) (Thamdrup et al., 2006). As N_2O is not supposed to be involved in the anammox process (Kartal et al., 2011),

anammox does not influence the N_2O distribution and only denitrification is thought to be responsible for N_2O consumption at suboxic to anoxic conditions (Bange, 2008). The widespread N_2O consumption in the OMZ core is thus an indicator for denitrification taking place in the ETSP (Farias et al., 2007). One explanation for these contradicting findings is that denitrification strongly depends on the supply of organic carbon or hydrogen sulfide (Chang et al., 2014;Dalsgaard et al., 2014;Galan et al., 2014).

As nitrification is one major process accompanying the remineralization of organic matter, a positive correlation between the excess N_2O (ΔN_2O) and the apparent oxygen utilization (AOU) is often interpreted as an indication for nitrification as the main N_2O production pathway (e.g. Walter et al. (2006), Forster et al. (2009)). An increase in the ΔN_2O/AOU ratio at low oxygen concentrations has been observed in several studies in different oceanic areas with reduced oxygen concentrations (Ryabenko et al., 2012;Upstill-Goddard et al., 1999;De Wilde and Helder, 1997), whereas a breakdown of this relationship due to N_2O consumption is observed when oxygen concentrations fall below a certain, not well defined, threshold (Zamora et al., 2012).

There is a strong indication that at low oxygen concentrations nitrification and denitrification may take place in close proximity (Kalvelage et al., 2011), and the N_2O production and consumption under these conditions are strongly influenced by the interaction of both processes. Stable isotope and consumption rate measurements of N_2O in oxygen-deficient waters indicated that N_2O accumulates within the oxycline as a result of the coupling between nitrification and denitrification whereas N_2O consumption in the OMZ core was associated with denitrification (Farias et al., 2007;Babbin et al., 2015). The exact oxygen concentration where N_2O consumption starts is not yet well determined, however (Cornejo and Farias, 2012;Zamora et al., 2012). Measurements of N_2O consumption rates in the eastern tropical North Pacific (ETNP) Ocean furthermore provided evidence for a rapid N_2O cycling within the ETNP, although depth profiles of N_2O seemed to be relatively invariant over time (Babbin et al., 2015). These quasi-stable conditions may be disturbed by rapid changes in the environmental conditions.

Although the waters off Peru harbor one of the most prominent OMZs in the world, only a few measurements of N_2O are available so far (Friederich et al., 1985;Nevison et al., 1995;Pierotti and Rasmussen, 1980), . N_2O measurements from the OMZ off Chile indicated the potential for high N_2O production and emissions due to the proximity of the OMZ to coastal upwelling taking place in this area (Charpentier et al., 2007;Castro-Gonzalez and Farias, 2004). Here we present N_2O measurements in the water column off Peru from six measurement campaigns in the ETSP. This upwelling area is one of the four major eastern boundary upwelling systems (EBUS) where alongshore trade winds induce westward transport of the surface water masses which leads to strong coastal upwelling (Chavez and Messié, 2009).The ETSP is characterized by one of the largest and most intense OMZs in the oceans, extending from the Peruvian shelf about 1000 km offshore with a maximum thickness of more than 600 m (Fuenzalida et al., 2009). It is located in the shadow zone of large ocean current systems which leads to a sluggish ventilation and long residence times of waters within the OMZ. To the North of the OMZ, equatorial current bands such as the Equatorial Undercurrent (EUC) and the Southern Subsurface Countercurrents (SSCC) supply waters to the ETSP which leads to slightly higher oxygen concentrations in the northern OMZ compared to the OMZ core (Stramma et al., 2010). The equatorial current bands also feed the poleward Peru-Chile Undercurrent (PCUC) which is the main source for waters upwelled along the coast where high primary production and high remineralization rates in the underlying waters lead to a further drawdown in oxygen concentrations (Karstensen et al., 2008). Active N loss can be observed in large parts of the OMZ which is reflected in a pronounced secondary nitrite maximum and a strong nitrogen deficit in the OMZ core (Codispoti et al., 1986). The OMZ extends over large parts of the Peruvian shelf where sulfidic conditions within the water column are frequently observed (Schunck et al., 2013). While year-round upwelling can be observed along the Peruvian coast, the region is strongly influenced by the El Niño Southern Oscillation (ENSO) leading to large interannual variability in the upwelling intensity which could lead to the interruption of the upwelling during El Niño events (Dewitte et al., 2012). While the OMZ core is largely unaffected by ENSO, a deepening of the upper oxycline and the re-oxygenation of the Peruvian shelf due to the propagation of coastal trapped waves can be observed (Gutierrez et al., 2008).

2 Methods

In total, 146 depth profiles (0-~4200 m) of N_2O were measured on two cruises between December 2008 and February 2009 (M77-3 & M77-4) and four cruises between October 2012 and March 2013 (M90 - M93) to the upwelling area and the adjacent open ocean off Peru onboard the German research vessel Meteor. The Southern Oscillation Indices (http://www.ncdc.noaa.gov/teleconnections/enso/indicators/soi/) from 2008/2009 and 2012/2013 did not indicate the presence of an El Niño event during our measurement campaigns, and similar conditions between both measurement campaigns could be expected. The locations of the sampled stations are shown in Fig. 1. While the M77-4 and M90 cruises mainly covered the open ocean area, the M77-3 and M91-M93 cruises mainly took place in the Peruvian shelf area. The work was part of the German DFG collaborative research project (SFB) 754 (https://www.sfb754.de/) and the BMBF project SOPRAN (Surface Ocean PRocesses in the Antropocene, www.sopran.pangaea.de). The N_2O data set described here has been archived in MEMENTO, the MarinE MethanE and NiTrous Oxide database (https://memento.geomar.de) (Kock and Bange, 2015).

Triplicate samples were taken from 10 L Niskin bottles mounted on a rosette water sampler or a pump-CTD (M77-3) in 25 ± 0.11 mL (M77-3 & M77-4) and 20 ± 0.14 mL (M90 - M93) opaque glass vials and sealed with butyl rubber stoppers and aluminum caps, thereby avoiding the inclusion of air bubbles.

Samples were treated with 0.2 mL (M77-3 & M77-4) and 0.05 mL (M90 - M93) of a saturated mercuric chloride solution directly after the sampling to inhibit microbial N_2O production or consumption. The samples were either analyzed onboard (M77-3 & M77-4, M91, partly M90 & M93) within a few days or shipped to GEOMAR by air freight for later analysis (M92, partly M90 & M93). Samples that were shipped to Germany were additionally sealed with paraffin wax and stored upside down to avoid the formation of air bubbles in the samples due to temperature and pressure changes during transportation.

Samples were analyzed using a static equilibration method: 10 mL helium (99.9999% AirLiquide, Düsseldorf, Germany) was manually injected into each vial which was equipped with a second syringe to collect the

147 overflowing water. Vials with added headspacewere vigorously shaken for about 20 s and allowed to
148 equilibrate at ambient temperature for a minimum of two hours. A subsample of the equilibrated headspace
149 was manually injected into a GC-ECD system (Hewlett-Packard 5890 Series II, Agilent Technologies, Santa Clara,
150 CA, USA), equipped with a 6' 1/8" packed column (molsieve, 5Å, W. R. Grace & Co.-Conn., Columbia, MY). The
151 GC was operated at 190 °C, using argon/methane (95%/5%, ECD purity, AirLiquide, Düsseldorf, Germany) as
152 carrier gas at a flow rate of 30 mL min^{-1}.

153 The GC was calibrated on a daily basis with a minimum of 2 (M77-3 & M77-4) or 4 (M90 - M93) different
154 standard gas mixtures (N_2O in synthetic air, Deuste-Steininger GmbH, Mühlhausen, Germany and Westfalen
155 AG, Münster, Germany). Standard gases were either injected as pure gas or further diluted with helium (1:3,
156 1:1 or 3:1) to obtain additional standard gas concentrations. Pure standard gaseswere calibrated against NOAA
157 primary standards at the Max Planck Institute for Biogeochemistry in Jena, Germany, if the standard gas
158 concentrations were within the calibration range of the NOAA gases. Gases with N_2O concentrations outside
159 the NOAA calibration range were internally calibrated using an LGR N_2O/CO analyzer (Los Gatos Research,
160 Mountain View, CA, USA), which was proven to have a linear response and minimal drift within the calibration
161 range (Arevalo-Martinez et al., 2013). The N_2O concentration in the samples was calculated according to Walter
162 et al. (2006) using the solubility function of Weiss and Price (1980). The average precision of the
163 measurements, calculated as median standard deviation from triplicate measurements, was 0.7 nM.

164 ΔN_2O was calculated as the difference between the in-situ concentration $[N_2O]_w$ and the equilibrium
165 concentration $[N_2O]_{eq}$:

166 $$\Delta N_2O = [N_2O]_w - [N_2O]_{eq} \qquad (1)$$

167 We used the contemporary atmospheric mixing ratio measured at Cape Grim, Tasmania
168 (http://agage.mit.edu/data/agage-data) for the calculation of $[N_2O]_{eq}$. This calculation underestimates the N_2O
169 excess in subsurface waters which have been isolated from the surface for a long time as it does not account

for the increase in the atmospheric mixing ratio since the beginning of the industrial revolution (Freing et al., 2009). The use of the contemporary N_2O mixing ratio of 2013 would lead to a maximum ~17% overestimate of $[N_2O]_{eq}$, thus leading to only a small error compared to the maximum N_2O concentrations measured in our study, and the use of the contemporary atmospheric mixing ratio still allows a qualitative analysis of the ΔN_2O/AOU relationship in order to investigate the formation and consumption processes of N_2O.

The potential temperature of the water parcel at a certain depth was calculated using the Gibbs Seawater Oceanographic Toolbox (McDougall and Barker, 2011).

Oxygen concentrations were measured either with a Seabird (M77-3 & M77-4: SBE-5; M90-M93: SBE 43) oxygen sensor (Sea-Bird Electronics, Bellevue, WA, USA) mounted on the CTD rosette or from 100 mL discrete samples taken from the Niskin bottles and analyzed using the Winkler titration method (Grasshoff et al., 1999). The oxygen sensor was calibrated against the Winkler measurements.

Recent studies using highly sensitive STOX (Switchable Trace amount Oxygen) sensors for oxygen measurements indicate that measurements with conventional oxygen sensors that are calibrated against Winkler measurements may be biased towards higher concentrations at near-zero oxygen conditions. Thamdrup et al. (Thamdrup et al., 2012) therefore argued that anoxic conditions are prevalent in the core of the Peruvian OMZ where oxygen concentrations of several µM have been found using the conventional Winkler-calibrated measurements. As STOX sensor measurements were not available for all measurement campaigns presented here, the minimum oxygen measurements reported here from the core of the OMZ (3-5 µM) should be considered as an overestimation.

The Apparent Oxygen Utilization (AOU) was calculated from the oxygen concentrations $[O_2]_w$ using the CSIRO SeaWater library, version 3.2 (http://www.cmar.csiro.au/datacentre/ext_docs/seawater.htm) to calculate oxygen saturation $[O_2]_{eq}$:

$$AOU = [O_2]_w - [O_2]_{eq} \qquad (2)$$

193 Nutrient samples from the CTD rosette were analyzed onboard following the nutrient analysis methods
194 according to Hansen et al. (1999). Samples taken from the pump-CTD during M77-3 were stored at -20°C and
195 shipped to Germany for later analysis. N' was calculated as a measure for the nitrogen deficit from the nitrate
196 ($[NO_3^-]$), nitrite ($[NO_2^-]$) and phosphate ($[PO_4^{3-}]$) concentrations as follows (Altabet et al., 2012):

197 $$N' = ([NO_3^-] + [NO_2^-]) - 16[PO_4^{3-}] \quad (3)$$

198 To distinguish between coastal and open ocean stations we calculated the distance of each station from the
199 continental slope (2000 m isobath) and used the first baroclinic Rossby radius of deformation as described by
200 Chelton et al. ((Chelton et al., 1998)) as threshold distance for stations that were influenced by coastal
201 upwelling.

202

3 Results and Discussion

The oxygen profiles revealed an intense oxygen minimum zone throughout the studied area, with a vertical thickness of several hundreds of meters. In the open ocean, the oxygen concentrations in the core of the OMZ increased towards the north from below 3 µM south of 5 °S to ~10 µM at the equator. South of 13°S the mixed layer depth significantly increased from ~50 m to ~100 m, which is reflected in the oxygen and N_2O distributions (Fig. 2). Due to the coastal upwelling, the depth of the upper OMZ boundary significantly decreased towards the coast, with a well oxygenated mixed layer of ~50 m in the open ocean and a mixed layer depth of less than 5 m on the shelf. Oxygen was strongly undersaturated in the surface waters on the shelf as a result of upwelling of waters from the underlying OMZ. Elevated phosphate concentrations in the surface waters at the coast also reflected the upwelling on the shelf (Fig. 3).

The vertical profiles showed characteristic nutrient distributions that marked the zones of nitrogen depletion: accumulation of nitrite was observed in the core of the OMZ where oxygen concentrations fell below ~5 µM and low N' values coincided with the nitrite maxima in the OMZ. The maximum nitrite concentration reached ~13 µM, with a more pronounced maximum at the shelf than in open ocean waters. Additionally, many profiles showed an additional, less pronounced primary nitrite maximum within the upper oxycline that is associated with nitrification (Codispoti and Christensen, 1985) (Fig. 4). At the shelf, strong signals of N loss throughout the water column are reflected in more negative N' and low nitrate values at the coast (Fig. 3).

The water mass distribution in our dataset agrees well with the data presented by Pietri et al. (2014) (Fig. 5). Due to the larger area covered by our measurements our data showed a broader scattering, but we could identify the same water masses in our data: below 500 m, both the coastal and the offshore profiles carry fresh (S~34.8) and cool (T_{pot}~5°C) Antarctic Intermediate Water (AAIW) (Pietri et al., 2014), while shallower subthermocline waters are covered by the Equatorial Subsurface Water (ESSW). Waters with low salinities (~34.6) and potential temperatures between 10°C and 15°C in the offshore waters can be traced back to Eastern South Pacific Intermediate Water (ESPIW) (Schneider et al., 2003). This water mass can hardly be

identified in the coastal data. Cold Coastal Water (CCW) with S ~15 and T_{pot} ~ 17°C could only be identified in the coastal data as it is directly related to the coastal upwelling, whereas the offshore surface data were associated with Subtropical Surface Water (STSW) (Pietri et al., 2013). The N_2O depth distribution showed a strong sensitivity to oxygen concentrations throughout the study area, and strong differences between coastal and offshore stations could be observed. In the offshore waters, surface N_2O concentrations were close to saturation, with a strong increase below the mixed layer (Fig. 2). Two types of depth profiles could be identified, reflecting marginal differences in the minimum oxygen concentrations observed in the OMZ: a broad N_2O maximum at the depth of the oxygen minimum was found at the northern and southern periphery of the oxygen minimum zone where the minimum oxygen concentrations did not fall below 5 µM. In contrast, N_2O depletion was found in the core of the OMZ, where oxygen concentrations below 5 µM were observed over a wide depth range. The N_2O depth profiles in the central OMZ thus revealed a double-peak structure with narrow N_2O maxima in the upper and lower oxycline (Fig. 4). This depth profile structure has been frequently observed in other oceanic areas with highly depleted oxygen concentrations (e.g.(Bange et al., 2010)). N_2O depletion coincided with nitrite accumulation in the OMZ core and high nitrate to phosphate ratios. In all offshore profiles N_2O concentrations did not exceed 80 nM.

A bilinear ΔN_2O/AOU relationship has been identified in the upper oxycline for waters with oxygen concentrations higher than 5 µM during the M77-4 cruise that took place in the offshore waters of the OMZ (Ryabenko et al., 2012). We found a very similar relationship for all offshore data with no systematic difference between the data from the M77-4 (January/February 2009) cruise and the M90 (November 2012) cruise (Figures 2, 6a). This indicates a comparable setting of the open ocean OMZ waters during both cruises. We furthermore found no difference in the ΔN_2O/AOU relationship between stations with a broad N_2O maximum and a double-peak structure. These results are similar to previously reported ΔN_2O/AOU relationships from other oceanic OMZs (Upstill-Goddard et al., 1999;Cohen and Gordon, 1978;De Wilde and Helder, 1997).The ΔN_2O distribution in the TS-diagram (Fig. 5) showed that elevated ΔN_2O values were mainly associated with

AAIW and ESSW, while surface waters were close to saturation. Compared to the offshore waters, the N_2O distribution on the shelf and in the adjacent deep waters showed a much larger variability. N_2O depletion was in fact observed at oxygen concentrations below 5 µM, too. While several N_2O profiles revealed a shape similar to the offshore profiles, an overall characteristic shape of the profiles could not be identified, however: profiles with a subsurface N_2O maximum in the oxycline were observed as well as profiles with multiple maxima or a surface N_2O maximum (Fig. 4). N_2O accumulation with concentrations which strongly exceeded the maximum offshore N_2O concentrations of 80 nM was frequently observed. Several profiles showed an extreme N_2O accumulation with concentrations up to ~850 nM (Fig. 4). The location and shape of the N_2O maxima in the different profiles was highly variable, which resulted in a very patchy distribution of N_2O in the water column over the shelf and in the adjacent waters (Fig. 3). This is also reflected in the TS-diagram of the coastal data (Fig.5), which showed that elevated ΔN_2O values were associated with CCW, but displayed a large variability within this water mass. High resolution measurements of surface N_2O during M90, M91 and M93 also revealed a very heterogeneous surface N_2O distribution with remarkably high concentrations of N_2O in vicinity of the main upwelling cells off Peru (Arevalo-Martinez et al., 2015).

In contrast to the open ocean waters, a correlation between ΔN_2O and AOU was not observed for the coastal data (Fig. 6b). The ΔN_2O/AOU ratio from the offshore waters serves as a lower limit for the coastal stations, where numerous values with much higher ΔN_2O/AOU ratios were observed. These data were highly scattered over the full range of oxygen concentrations, indicating that for the coastal stations the N_2O maxima were not associated with suboxic conditions as observed offshore. The ΔN_2O values that showed the strongest deviation from the offshore ΔN_2O/AOU ratio were associated with highly negative N' values as a signal for a large nitrogen deficit (Fig. 6b). This indicates that these waters with extreme N_2O accumulation had been subject to extensive N loss.

Extreme accumulation of N_2O with concentrations up to 765 nM in the oceanic water column has also been found in the Arabian Sea (Naqvi et al., 2010;Naqvi et al., 2006) and at a time series station off Chile (Farías et al., 2015), where maximum concentrations of ~500 nM were found. Naqvi et al. (2000) explained the extreme N_2O accumulation over the Indian shelf with the response of denitrifying enzymes to transient oxygen depletion. N_2O thus accumulated when waters reached suboxic conditions. N_2O accumulation coincided with the accumulation of nitrite and consumption of N_2O started when these waters became sulfidic (Naqvi et al., 2010). Farías et al. (2015) measured N_2O accumulation during the transition from oxic to anoxic conditions, too, but at variable oxygen concentrations whereas N_2O depletion became dominant under suboxic conditions. In contrast to the results from the Indian Ocean, they identified enhanced remineralization due to short-term variability in coastal upwelling as the main driver for N_2O accumulation.

In our study, N_2O accumulation did not coincide with the accumulation of nitrite. N_2O was generally depleted in samples that showed marked nitrite accumulation (Fig. 4) and similar to the measurements off Chile, we found strongly elevated N_2O concentrations (>100 nM) over the full range of oxygen concentrations (Fig. 5), whereas N_2O accumulation on the Indian shelf was restricted to suboxic conditions.

The high oxygen concentrations found in the majority of our samples with extreme N_2O accumulation excludes in-situ denitrification or anammox (see e.g. Babbin et al. (2014), Dalsgaard et al. (2014)). The extraordinarily high N_2O concentrations as well as the low N' values thus have to be old signals of processes taking place under anoxic to suboxic conditions. There is no known consumption process for N_2O in oxygenated waters (Bange, 2008), and the strong signals of N loss that are produced under anoxic conditions are unlikely to be rapidly compensated by N fixation upon oxygenation. Both signals thus are likely to have remained preserved when oxygen concentrations increased due to (diapycnal or isopycnal) mixing with waters of higher oxygen concentration or due to direct contact with the atmosphere as a result of upwelling. Our observations of high N_2O concentrations in oxygenated waters furthermore indicate that this accumulation could have taken place during re-oxygenation rather than during decreasing oxygen concentrations. An increase in oxygen

298 concentrations would lead to the preservation of the high N_2O signals in the water column whereas further
299 decreasing oxygen concentrations would only lead to a temporal N_2O accumulation and would eventually
300 stimulate N_2O consumption.

301 Enhanced production of N_2O after transition from anoxic to oxic conditions is a known process occurring in
302 soils (e.g. Morley et al. (2008)) and may be explained by different sensitivity of denitrifying enzymes to trace
303 concentrations of oxygen (Tiedje, 1988). In a recent incubation study, Dalsgaard et al. (2014) found no
304 indication for an increased N_2O production by denitrification due to changes in the oxygen concentration at
305 nanomolar levels, however. Instead, autotrophic denitrification and N_2O production have been shown to be
306 stimulated by the addition of hydrogen sulfide (H_2S) (Galan et al., 2014;Dalsgaard et al., 2014). We did not find
307 direct evidence for a coupling between N_2O production and the presence of H_2S in our measurements, as high
308 N_2O accumulation was often found in proximity to H_2S plumes but was also detected when H_2S was absent in
309 the water column. We cannot exclude that the high N_2O production we frequently observed at the shelf is
310 stimulated by a coupling of denitrification with sulfur cycling, though: Canfield et al. (2010) found evidence for
311 active sulfur cycling in the ETSP without H_2S accumulation, and a coupling between H_2S oxidation and
312 denitrification has been shown before (Galan et al., 2014;Jensen et al., 2009). Indeed, active denitrification was
313 found in proximity to H_2S plumes in the water column during M77-3 (Kalvelage et al., 2013;Schunck et al.,
314 2013).

315 In the ocean, increased N_2O production was also associated with the onset of nitrification after re-ventilation
316 of the water column in a seasonal study in the Baltic Sea, but with relatively low resulting N_2O concentrations
317 (Naqvi et al., 2010). Yu et al. (2010) found strongly increased N_2O production by nitrifying bacteria that was
318 stimulated by the availability of ammonium during recovery from anoxic conditions in a chemostat culture
319 experiment. Their results point towards an increased N_2O production via the ammonium-oxidation pathway,
320 while N_2O production by nitrifier-denitrification seemed not to be stimulated by the shift from anoxic to oxic
321 conditions. We frequently measured high ammonium concentrations along the Peruvian shelf, indeed (Fig. 4),

322 which could have stimulated N_2O production from ammonium oxidation. A direct correlation between N_2O and
323 ammonium could not be identified, however. From our concentration measurements alone we thus cannot
324 distinguish if the observed high production of N_2O is a result of denitrification or nitrification processes. Studies
325 of the isotopic and isotopomeric N_2O composition could reveal more detailed insights whether N_2O is produced
326 via the ammonium oxidation or the nitrite reduction pathway during extreme accumulation.

327 Together with the high N_2O concentrations we found low N' values that were associated with oxygenated
328 waters only at the shelf, whereas in the open ocean N depletion was restricted to the OMZ core (Fig. 6). This
329 could indicate that the re-oxygenation of the oxygen-deficient waters mainly happens at the shelf, whereas
330 waters in the open ocean OMZ are less affected by mixing processes. Strong diapycnal and isopycnal mixing on
331 the shelf has indeed been reported from the Peruvian and Mauritanian upwelling region (Schafstall et al., 2010;
332 Thomsen et al., JGR, submitted, 2015, (Pietri et al., 2014)).

333 The upwelling-induced high primary production in the surface ocean furthermore fuels rapid oxygen
334 consumption in the underlying waters due to the export and remineralization of organic matter, thereby
335 creating strong small-scale variability in oxygen concentrations. Kalvelage et al. (2013) showed that these high
336 remineralization rates also induce strong N cycling in the subsurface layer. Turnover rates for different N
337 species are therefore much faster on the shelf than in the open ocean OMZ (Hu et al., 2015),which is also
338 reflected in the distribution of different functional gene abundances (Loescher et al., 2014). One factor that
339 also contributes to the N_2O accumulation on the shelf could thus be generally higher rates of nitrification
340 and/or denitrification on the shelf than in the open ocean.

341

4 Summary and Conclusions

We observed extreme N_2O accumulations over the Peruvian shelf and in the adjacent waters with maximum concentrations similar to the observations made by Naqvi et al. (2000) over the Indian shelf and Farías et al. (2015) off Chile, whereas N_2O concentrations in the open ocean OMZ off Peru were comparably moderate.

We found strong evidence that N_2O accumulations are preserved when oxygen concentrations increased as a result of mixing and exchange with the overlying atmosphere in the upwelling zone. Waters with high N_2O concentrations can thus be directly and frequently transported to the surface ocean. This makes this region one of the most important oceanic regions for N_2O emissions to the atmosphere (Arevalo-Martinez et al., 2015). This direct link between unusually high N_2O production and emissions over the Peruvian shelf makes it necessary to understand the biogeochemical processes involved in N_2O production and consumption to produce reliable predictions of oceanic emissions from this area. Current approaches to model the N_2O distribution rely on parameterizations based on the linear ΔN_2O/AOU relationship (Suntharalingam and Sarmiento, 2000;Nevison et al., 2003;Freing et al., 2012). These approaches could in fact reproduce the oxygen distribution in the open ocean OMZ off Peru reasonably well, but they fail to account for the extreme N_2O accumulation and its high spatial and temporal variability over the shelf area. They thus significantly underestimate the emissions from the Peruvian upwelling and potentially other upwelling areas with similar conditions, too.

Acknowledgements

We would like to thank the captains and crew of the R/V Meteor for their professional support and the chief scientists of M77-3 & M90-M93, Martin Frank, Lothar Stramma, Stefan Sommer and Gaute Lavik for the opportunity to collect samples during their cruises. We would also like to thank Annie Bourbonnais and Johanna Maltby for the collection of N_2O samples during M92, and Gesa Eirund, Joel Craig, Georgina Flores, Jennifer Zur, Moritz Baumann, Tina Baustian and Dörte Nitschkowski for their help in analyzing the samples.

We would like to thank Frank Malien, Mirja Dunker, Violeta Leon, Peter Fritsche, Tina Baustian, Kerstin Nachtigall, Martina Lohmann, Gabriele Klockgether and Tim Kalvelage for the sampling and analysis of oxygen and nutrient samples during M77-3 & M77-4 and M90-M93. The work presented here was made possible by the DFG-supported projects SFB754 Phase I and II (http://www.sfb754.de) and the BMBF joint projects SOPRAN II and III (FKZ 03F0611A and FKZ 03F662A).

References

Altabet, M. A., Ryabenko, E., Stramma, L., Wallace, D. W. R., Frank, M., Grasse, P., and Lavik, G.: An eddy-stimulated hotspot for fixed nitrogen-loss from the Peru oxygen minimum zone, Biogeosciences, 9, 4897-4908, 10.5194/bg-9-4897-2012, 2012.

Arevalo-Martinez, D. L., Beyer, M., Krumbholz, M., Piller, I., Kock, A., Steinhoff, T., Kortzinger, A., and Bange, H. W.: A new method for continuous measurements of oceanic and atmospheric N2O, CO and CO2: performance of off-axis integrated cavity output spectroscopy (OA-ICOS) coupled to non-dispersive infrared detection (NDIR), Ocean Science, 9, 1071-1087, 10.5194/os-9-1071-2013, 2013.

Arevalo-Martinez, D. L., Kock, A., Löscher, C. R., Schmitz, R. A., and Bange, H. W.: Massive nitrous oxide emissions from the tropical South Pacific Ocean, Nature Geosci, 8, 530-533, 10.1038/ngeo2469 http://www.nature.com/ngeo/journal/vaop/ncurrent/abs/ngeo2469.html#supplementary-information, 2015.

Babbin, A. R., Keil, R. G., Devol, A. H., and Ward, B. B.: Organic Matter Stoichiometry, Flux, and Oxygen Control Nitrogen Loss in the Ocean, Science, 344, 406-408, 10.1126/science.1248364, 2014.

Babbin, A. R., Bianchi, D., Jayakumar, A., and Ward, B. B.: Rapid nitrous oxide cycling in the suboxic ocean, Science, 348, 1127-1129, 10.1126/science.aaa8380, 2015.

Bange, H. W.: Air-sea exchange of nitrous oxide and methane in the Arabian Sea: A simple model of the seasonal variability, Indian Journal of Marine Sciences, 33, 77-83, 2004.

Bange, H. W.: Gaseous nitrogen compounds (NO,N2O,N2,NH3) in the ocean, in: Nitrogen in the Marine Environment, 2 ed., edited by: Capone, D. G., Bronk, D. A., Mulholland, M. R., and Carpenter, E. J., Academic Press/Elsevier 51-94, 2008.

Bange, H. W., Freing, A., Kock, A., and Löscher, C. R.: Marine pathways to nitrous oxide, in: Nitrous Oxide and Climate Change, edited by: Smith, K., Earthscan, London, 36-62, 2010.

Canfield, D. E., Stewart, F. J., Thamdrup, B., De Brabandere, L., Dalsgaard, T., Delong, E. F., Revsbech, N. P., and Ulloa, O.: A Cryptic Sulfur Cycle in Oxygen-Minimum-Zone Waters off the Chilean Coast, Science, 330, 1375-1378, 10.1126/science.1196889, 2010.

Castro-Gonzalez, M., and Farias, L.: N(2)O cycling at the core of the oxygen minimum zone off northern Chile, Marine Ecology-Progress Series, 280, 1-11, 10.3354/meps280001, 2004.

Chang, B. X., Rich, J. R., Jayakumar, A., Naik, H., Pratihary, A. K., Keil, R. G., Ward, B. B., and Devol, A. H.: The effect of organic carbon on fixed nitrogen loss in the eastern tropical South Pacific and Arabian Sea oxygen deficient zones, Limnology and Oceanography, 59, 1267-1274, 10.4319/lo.2014.59.4.1267, 2014.

Charpentier, J., Farias, L., Yoshida, N., Boontanon, N., and Raimbault, P.: Nitrous oxide distribution and its origin in the central and eastern South Pacific Subtropical Gyre, Biogeosciences, 4, 729-741, 10.5194/bg-4-729-2007, 2007.

Charpentier, J., Farias, L., and Pizarro, O.: Nitrous oxide fluxes in the central and eastern South Pacific, Global Biogeochemical Cycles, 24, -, Artn Gb3011
Doi 10.1029/2008gb003388, 2010.

Chavez, F. P., and Messié, M.: A comparison of Eastern Boundary Upwelling Ecosystems, Prog. Oceanogr., 83, 80-96, 2009.

Chelton, D. B., DeSzoeke, R. A., Schlax, M. G., El Naggar, K., and Siwertz, N.: Geographical variability of the first baroclinic Rossby radius of deformation, Journal of Physical Oceanography, 28, 433-460, 10.1175/1520-0485(1998)028<0433:gvotfb>2.0.co;2, 1998.

Ciais, P., Sabine, C. L., Bala, G., Bopp, L., Brovkin, V., Canadell, J., Chhabra, A., DeFries, R., Galloway, J. N., Heimann, M., Jones, C., Le Quéré, C., Myneni, R., Piao, S., and Thornton, P.: Carbon and other Biogeochemical Cycles, in: Climate Change 2013: The Physical Science Basis. Contribution of Working Group I to the Fifth Assessment Report of the Intergovernmental Panel on Climate Change, edited by: Stocker, T. F., Qin, D., Plattner, G.-K., Tignor, M., Allen, S. K., Boschung, J., Nauels, A., Xia, Y., Bex, V., and Midgley, P. M., Cambridge University Press, Cambridge, UK, and New York, NY, USA, 465-570, 2013.

Codispoti, L. A., and Christensen, J. P.: Nitrification, denitrification and nitrous oxide cycling in the eastern tropical South Pacific Ocean, Marine Chemistry, 16, 277-300, 1985.

Codispoti, L. A., Friederich, G. E., Packard, T. T., Glover, H. E., Kelly, P. J., Spinrad, R. W., Barber, R. T., Elkins, J. W., Ward, B. B., Lipschultz, F., and Lostaunau, N.: High nitrite levels off northern Peru: A signal of instability in the marine denitrification rate, Science, 233, 1200-1202, 1986.

Cohen, Y., and Gordon, L. I.: Nitrous oxide in oxygen minimum of eastern tropical North Pacific - evidence for its consumption during denitrification and possible mechanisms for its production, Deep-Sea Research, 25, 509-524, 10.1016/0146-6291(78)90640-9, 1978.

Cornejo, M., and Farias, L.: Following the N2O consumption in the oxygen minimum zone of the eastern South Pacific, Biogeosciences, 9, 3205-3212, 10.5194/bg-9-3205-2012, 2012.

Dalsgaard, T., Stewart, F. J., Thamdrup, B., De Brabandere, L., Revsbech, N. P., Ulloa, O., Canfield, D. E., and DeLong, E. F.: Oxygen at Nanomolar Levels Reversibly Suppresses Process Rates and Gene Expression in Anammox and Denitrification in the Oxygen Minimum Zone off Northern Chile, Mbio, 5, UNSP e01966 10.1128/mBio.01966-14, 2014.

De Wilde, H. P. J., and Helder, W.: Nitrous oxide in the Somali Basin: the role of upwelling, Deep Sea Research Part II: Topical Studies in Oceanography, 44, 1319-1340, http://dx.doi.org/10.1016/S0967-0645(97)00011-8, 1997.

Deutsch, C., Sarmiento, J. L., Sigman, D. M., Gruber, N., and Dunne, J. P.: Spatial coupling of nitrogen inputs and losses in the ocean, Nature, 445, 163-167, 10.1038/nature05392, 2007.

Dewitte, B., Vazquez-Cuervo, J., Goubanova, K., Illig, S., Takahashi, K., Cambon, G., Purca, S., Correa, D., Gutierrez, D., Sifeddine, A., and Ortlieb, L.: Change in El Nino flavours over 1958-2008: Implications for the long-term trend of the upwelling off Peru, Deep-Sea Res Pt Ii, 77-80, 143-156, 10.1016/j.dsr2.2012.04.011, 2012.

Farias, L., Paulmier, A., and Gallegos, M.: Nitrous oxide and N-nutrient cycling in the oxygen minimum zone off northern Chile, Deep-Sea Research Part I-Oceanographic Research Papers, 54, 164-180, 10.1016/j.dsr.2006.11.003, 2007.

Farías, L., Besoain, V., and García-Loyola, S.: Presence of nitrous oxide hotspots in the coastal upwelling area off central Chile: an analysis of temporal variability based on ten years of a biogeochemical time series, Environmental Research Letters, 10, 044017, 10.1088/1748-9326/10/4/04, 2015.

Fernandez, C., Farias, L., and Ulloa, O.: Nitrogen Fixation in Denitrified Marine Waters, Plos One, 6, e20539 10.1371/journal.pone.0020539, 2011.

Firestone, M. K., Firestone, R. B., and Tiedje, J. M.: Nitrous-oxide from soil denitrification - factors controlling its biological production, Science, 208, 749-751, 10.1126/science.208.4445.749, 1980.

Forster, G., Upstill-Goddard, R. C., Gist, N., Robinson, C., Uher, G., and Woodward, E. M. S.: Nitrous oxide and methane in the Atlantic Ocean between 50 degrees N and 52 degrees S: Latitudinal distribution and sea-to-air flux, Deep-Sea Res Pt Ii, 56, 964-976, 10.1016/j.dsr2.2008.12.002, 2009.

Frame, C. H., and Casciotti, K. L.: Biogeochemical controls and isotopic signatures of nitrous oxide production by a marine ammonia-oxidizing bacterium, Biogeosciences, 7, 2695-2709, DOI 10.5194/bg-7-2695-2010, 2010.

Freing, A., Wallace, D. W. R., Tanhua, T., Walter, S., and Bange, H. W.: North Atlantic production of nitrous oxide in the context of changing atmospheric levels, Global Biogeochem. Cycles, 23, 10.1029/2009gb003472, 2009.

Freing, A., Wallace, D. W. R., and Bange, H. W.: Global oceanic production of nitrous oxide, Philosophical Transactions of the Royal Society B-Biological Sciences, 367, 1245-1255, 10.1098/rstb.2011.0360, 2012.

Friederich, G. E., Kelly, P. J., Codispoti, L. A., Spinrad, R. W., Kullenberg, G., Elkins, J. W., Kogelschatz, J., Packard, T. T., Lipschultz, F., Glover, H. E., Ward, B. B., and Smith, A. E.: Microbial nitrogen transformations in the oxygen minimum zone off Peru., Bigelow Laboratory for Ocean Sciences, East Boothbay, ME, 1985.

Fuenzalida, R., Schneider, W., Garcés-Vargas, J., Bravo, L., and Lange, C.: Vertical and horizontal extension of the oxygen minimum zone in the eastern South Pacific Ocean, Deep Sea Research Part II: Topical Studies in Oceanography, 56, 992-1003, 2009.

Galan, A., Faundez, J., Thamdrup, B., Francisco Santibanez, J., and Farias, L.: Temporal dynamics of nitrogen loss in the coastal upwelling ecosystem off central Chile: Evidence of autotrophic denitrification through sulfide oxidation, Limnology and Oceanography, 59, 1865-1878, 10.4319/lo.2014.59.6.1865, 2014.

Goreau, T. J., Kaplan, W. A., Wofsy, S. C., McElroy, M. B., Valois, F. W., and Watson, S. W.: Production of NO_2^- and N_2O by nitrifying bacteria at reduced concentrations of oxygen, Appl. Environ. Microbiol., 40, 526-532, 1980.

Gutierrez, D., Enriquez, E., Purca, S., Quipuzcoa, L., Marquina, R., Flores, G., and Graco, M.: Oxygenation episodes on the continental shelf of central Peru: Remote forcing and benthic ecosystem response, Prog. Oceanogr., 79, 177-189, 10.1016/j.pocean.2008.10.025, 2008.

Hamersley, M. R., Lavik, G., Woebken, D., Rattray, J. E., Lam, P., Hopmans, E. C., Sinninghe Damste, J. S., Krueger, S., Graco, M., Gutierrez, D., and Kuypers, M. M. M.: Anaerobic ammonium oxidation in the Peruvian oxygen minimum zone, Limnology and Oceanography, 52, 923-933, 2007.

Hansen, H. P., and Koroleff, F.: Determination of nutrients, in: Methods of seawater analysis, edited by: Grasshoff, K., Kremling, K., and Ehrhardt, M., Wiley-VCH, Weinheim, 159-228, 1999.

Hu, H., Bourbonnais, A., Larkum, J., Bange, H. W., and Altabet, M. A.: Nitrogen cycling in shallow low oxygen coastal waters off Peru from nitrite and nitrate nitrogen and oxygen isotopes, Biogeosciences Discuss., 12, 7257-7299, 10.5194/bgd-12-7257-2015, 2015.

IPCC: Climate Change 2013: The Physical Science Basis. Contribution of Working Group I to the Fifth Assessment Report of the Intergovernmental Panel on Climate Change., Cambridge, UK and New York, NY, 1535, 2013.

Jensen, M. M., Petersen, J., Dalsgaard, T., and Thamdrup, B.: Pathways, rates, and regulation of N-2 production in the chemocline of an anoxic basin, Mariager Fjord, Denmark, Marine Chemistry, 113, 102-113, 10.1016/j.marchem.2009.01.002, 2009.

Kalvelage, T., Jensen, M. M., Contreras, S., Revsbech, N. P., Lam, P., Guenter, M., LaRoche, J., Lavik, G., and Kuypers, M. M. M.: Oxygen Sensitivity of Anammox and Coupled N-Cycle Processes in Oxygen Minimum Zones, Plos One, 6, e29299
10.1371/journal.pone.0029299, 2011.

Kalvelage, T., Lavik, G., Lam, P., Contreras, S., Arteaga, L., Loescher, C. R., Oschlies, A., Paulmier, A., Stramma, L., and Kuypers, M. M. M.: Nitrogen cycling driven by organic matter export in the South Pacific oxygen minimum zone, Nature Geoscience, 6, 228-234, 10.1038/ngeo1739, 2013.

Karstensen, J., Stramma, L., and Visbeck, M.: Oxygen minimum zones in the eastern tropical Atlantic and Pacific oceans, Prog. Oceanogr., 77, 331-350, 10.1016/j.pocean.2007.05.009, 2008.

503 Kartal, B., Maalcke, W. J., de Almeida, N. M., Cirpus, I., Gloerich, J., Geerts, W., den Camp, H., Harhangi, H. R.,
504 Janssen-Megens, E. M., Francoijs, K. J., Stunnenberg, H. G., Keltjens, J. T., Jetten, M. S. M., and Strous, M.:
505 Molecular mechanism of anaerobic ammonium oxidation, Nature, 479, 127-U159, 10.1038/nature10453, 2011.

506 Kock, A., and Bange, H. W.: Counting the ocean's greenhouse gas emissions, Eos, 96, 10-13,
507 10.1029/2015EO023665, 2015.

508 Loescher, C. R., Grosskopf, T., Desai, F. D., Gill, D., Schunck, H., Croot, P. L., Schlosser, C., Neulinger, S. C.,
509 Pinnow, N., Lavik, G., Kuypers, M. M. M., LaRoche, J., and Schmitz, R. A.: Facets of diazotrophy in the oxygen
510 minimum zone waters off Peru, Isme Journal, 8, 2180-2192, 10.1038/ismej.2014.71, 2014.

511 Löscher, C. R., Kock, A., Könneke, M., LaRoche, J., Bange, H. W., and Schmitz, R. A.: Production of oceanic
512 nitrous oxide by ammonia-oxidizing archaea, Biogeosciences, 9, 2419-2429, 10.5194/bg-9-2419-2012, 2012.

513 Morley, N., Baggs, E. M., Dorsch, P., and Bakken, L.: Production of NO, N(2)O and N(2) by extracted soil
514 bacteria, regulation by NO(2)(-) and O(2) concentrations, FEMS Microbiol. Ecol., 65, 102-112, 10.1111/j.1574-
515 6941.2008.00495.x, 2008.

516 Naqvi, S. W. A., Jayakumar, D. A., Narveka, P. V., Naik, H., Sarma, V. V. S. S., D'Souza, W., Joseph, S., and
517 George, M. D.: Increased marine production of N_2O due to intensifying anoxia on the Indian continental shelf,
518 Nature, 408, 346-349, 2000.

519 Naqvi, S. W. A., Naik, H., Pratihary, A., D'Souza, W., Narvekar, P. V., Jayakumar, D. A., Devol, A. H., Yoshinari, T.,
520 and Saino, T.: Coastal versus open-ocean denitrification in the Arabian Sea, Biogeosciences, 3, 621-633, 2006.

521 Naqvi, S. W. A., Bange, H. W., Farias, L., Monteiro, P. M. S., Scranton, M. I., and Zhang, J.: Marine
522 hypoxia/anoxia as a source of CH4 and N2O, Biogeosciences, 7, 2159-2190, 10.5194/bg-7-2159-2010, 2010.

523 Nevison, C., Butler, J. H., and Elkins, J. W.: Global distribution of N2O and the Delta N2O-AOU yield in the
524 subsurface ocean, Global Biogeochemical Cycles, 17, 1119
525 10.1029/2003gb002068, 2003.

526 Nevison, C. D., Weiss, R. F., and Erickson, D. J.: Global oceanic emissions of nitrous oxide, Journal of
527 Geophysical Research-Oceans, 100, 15809-15820, 10.1029/95JC00684, 1995.

528 Nevison, C. D., Lueker, T. J., and Weiss, R. F.: Quantifying the nitrous oxide source from coastal upwelling,
529 Global Biogeochem. Cycles, 18, GB1018
530 10.1029/2003GB002110, 2004.

Ni, B.-J., Peng, L., Law, Y., Guo, J., and Yuan, Z.: Modeling of Nitrous Oxide Production by Autotrophic Ammonia-Oxidizing Bacteria with Multiple Production Pathways, Environmental Science & Technology, 48, 3916-3924, 10.1021/es405592h, 2014.

Pierotti, D., and Rasmussen, R. A.: Nitrous-Oxide Measurements in the Eastern Tropical Pacific-Ocean, Tellus, 32, 56-72, 1980.

Pietri, A., Testor, P., Echevin, V., Chaigneau, A., Mortier, L., Eldin, G., and Grados, C.: Finescale Vertical Structure of the Upwelling System off Southern Peru as Observed from Glider Data, Journal of Physical Oceanography, 43, 631-646, 10.1175/jpo-d-12-035.1, 2013.

Pietri, A., Echevin, V., Testor, P., Chaigneau, A., Mortier, L., Grados, C., and Albert, A.: Impact of a coastal-trapped wave on the near-coastal circulation of the Peru upwelling system from glider data, Journal of Geophysical Research-Oceans, 119, 2109-2120, 10.1002/2013jc009270, 2014.

Ryabenko, E., Kock, A., Bange, H. W., Altabet, M. A., and Wallace, D. W. R.: Contrasting biogeochemistry of nitrogen in the Atlantic and Pacific Oxygen Minimum Zones, Biogeosciences, 9, 203-215, 10.5194/bg-9-203-2012, 2012.

Santoro, A. E., Buchwald, C., McIlvin, M. R., and Casciotti, K. L.: Isotopic Signature of N(2)O Produced by Marine Ammonia-Oxidizing Archaea, Science, 333, 1282-1285, 10.1126/science.1208239, 2011.

Schafstall, J., Dengler, M., Brandt, P., and Bange, H.: Tidal-induced mixing and diapycnal nutrient fluxes in the Mauritanian upwelling region, J. Geophys. Res. - Oceans, 115, C10014 10.1029/2009jc005940, 2010.

Schneider, W., Fuenzalida, R., Rodriguez-Rubio, E., Garces-Vargas, J., and Bravo, L.: Characteristics and formation of eastern South Pacific intermediate water, Geophysical Research Letters, 30, 1581 10.1029/2003gl017086, 2003.

Schunck, H., Lavik, G., Desai, D. K., Grosskopf, T., Kalvelage, T., Loescher, C. R., Paulmier, A., Contreras, S., Siegel, H., Holtappels, M., Rosenstiel, P., Schilhabel, M. B., Graco, M., Schmitz, R. A., Kuypers, M. M. M., and LaRoche, J.: Giant Hydrogen Sulfide Plume in the Oxygen Minimum Zone off Peru Supports Chemolithoautotrophy, Plos One, 8, e68661 10.1371/journal.pone.0068661, 2013.

Stein, L. Y.: Surveying N_2O-producing pathways in bacteria, in: Methods in Enzymology: Research on Nitrification and Related Processes, Vol 486, Part A, edited by: Klotz, M. G., Methods in Enzymology, 131-152, 2011.

Stieglmeier, M., Mooshammer, M., Kitzler, B., Wanek, W., Zechmeister-Boltenstern, S., Richter, A., and Schleper, C.: Aerobic nitrous oxide production through N-nitrosating hybrid formation in ammonia-oxidizing archaea, Isme Journal, 8, 1135-1146, 10.1038/ismej.2013.220, 2014.

Stramma, L., Johnson, G. C., Firing, E., and Schmidtko, S.: Eastern Pacific oxygen minimum zones: Supply paths and multidecadal changes, Journal of Geophysical Research-Oceans, 115, C09011 10.1029/2009jc005976, 2010.

Suntharalingam, P., and Sarmiento, J. L.: Factors governing the oceanic nitrous oxide distribution: Simulations with an ocean general circulation model, Global Biogeochemical Cycles, 14, 429-454, 10.1029/1999gb900032, 2000.

Thamdrup, B., Dalsgaard, T., Jensen, M. M., Ulloa, O., Farias, L., and Escribano, R.: Anaerobic ammonium oxidation in the oxygen-deficient waters off northern Chile, Limnology and Oceanography, 51, 2145-2156, 2006.

Thamdrup, B., Dalsgaard, T., and Revsbech, N. P.: Widespread functional anoxia in the oxygen minimum zone of the Eastern South Pacific, Deep-Sea Research Part I-Oceanographic Research Papers, 65, 36-45, 10.1016/j.dsr.2012.03.001, 2012.

Tiedje, J. M.: Ecology of denitrification and dissimilatory nitrate reduction to ammonium, in: Biology of anearobic microorganisms, edited by: Zehnder, A. J. B., Wiley & Sons, New York, 179-244, 1988.

Upstill-Goddard, R. C., Barnes, J., and Owens, N. J. P.: Nitrous oxide and methane during the 1994 SW monsoon in the Arabian Sea/northwestern Indian Ocean, Journal of Geophysical Research-Oceans, 104, 30067-30084, 10.1029/1999jc900232, 1999.

Voss, M., and Montoya, J. P.: NITROGEN CYCLE Oceans apart, Nature, 461, 49-50, 10.1038/461049a, 2009.

Walter, S., Bange, H. W., Breitenbach, U., and Wallace, D. W. R.: Nitrous oxide in the North Atlantic Ocean, Biogeosciences, 3, 607-619, 10.5194/bg-3-607-2006, 2006.

Ward, B. B., Devol, A. H., Rich, J. J., Chang, B. X., Bulow, S. E., Naik, H., Pratihary, A., and Jayakumar, A.: Denitrification as the dominant nitrogen loss process in the Arabian Sea, Nature, 461, 78-U77, 10.1038/nature08276, 2009.

Weiss, R. F., and Price, B. A.: Nitrous oxide solubility in water and seawater, Mar. Chem., 8, 347-359, 1980.

WMO: Scientific Assessment of Ozone Depletion: 2010, Global Ozone Research and Monitoring Project, Geneva, Switzerland, 2011.

Yu, R., Kampschreur, M. J., Loosdrecht, M. C. M. v., and Chandran, K.: Mechanisms and Specific Directionality of Autotrophic Nitrous Oxide and Nitric Oxide Generation during Transient Anoxia, Environmental Science & Technology, 44, 1313-1319, 10.1021/es902794a, 2010.

Zamora, L. M., Oschlies, A., Bange, H. W., Huebert, K. B., Craig, J. D., Kock, A., and Loscher, C. R.: Nitrous oxide dynamics in low oxygen regions of the Pacific: insights from the MEMENTO database, Biogeosciences, 9, 5007-5022, 10.5194/bg-9-5007-2012, 2012.

599 Figures:

600 Figure 1: Station maps of the sampled N_2O stations from cruises A) M77-3, December 2008 – January 2009 (●)
601 and M77-4, January – February 2009 (⊙), B) M90, November 2012 (●) and M91, December 2012 (⊙), C)
602 M92, January 2013 (●) and M93, February – March 2013 (⊙). Section annotations in A) and B) correspond to
603 the vertical sections shown in Fig. 2 and 3.

604 Figure 2: Spatial distributions of oxygen (A, B), nitrite (C, D) and N_2O (E, F) along 86°W during M77-4 (2009, A, C,
605 E) and M90 (2012, B, D, F). Small dots indicate location and depth of the discrete samples. Data gridding:
606 ODV/DIVA.

607 Figure 3: Cross-shelf distribution of A) Oxygen, B) Phosphate, C) Nitrate, D) N', e) Nitrite and f) N_2O during M91
608 (Section F).

609 Figure 4: Selected depth profiles of oxygen (black dots, dotted line), sigma-theta (grey line) and N_2O (red line,
610 open circles) (left panel) and nitrate (grey line), nitrite (black circles, dotted line), ammonium (blue
611 diamonds, straight line) and N' (red line, small dots) (right panel) from selected open ocean and shelf
612 stations during M90-93. Depth profiles of oxygen and sigma-theta were taken from the CTD sensors, the
613 other parameters are taken from discrete samples. The locations of the respective stations are shown in the
614 map. Red signals denote stations classified as "coastal" stations whereas blue signals denote "offshore"
615 stations. Please note the changes in the scales for N_2O, sigma-theta, nitrite and ammonium.

616 Figure 5: Temperature-Salinity diagrams with ΔN_2O color coded for a) the offshore stations and b) the onshore
617 stations. Different symbols denote different cruises: ☆M77-3; ◊ M77-4; ○ M92; ▷M90; ◁ M91; ✳M93.

618 Figure 6: ΔN_2O/AOU relationship from a) offshore stations and b) coastal stations. Samples from the upper
619 OMZ and oxycline (sample depth < 350 m) are color coded with N'. Different symbols for different cruises
620 are denoted the same as in Figure 5. The black line denotes the ΔN_2O/AOU relationship from the offshore

621 data for samples with O2>50 µM and depth < 350 m (y=0.13x+3.73; r^2=0.83). Please note the change in the

622 scaling for ΔN_2O values of 0 - 100 nM and 100 - 1000 nM (dotted line).

623 Figure 1:

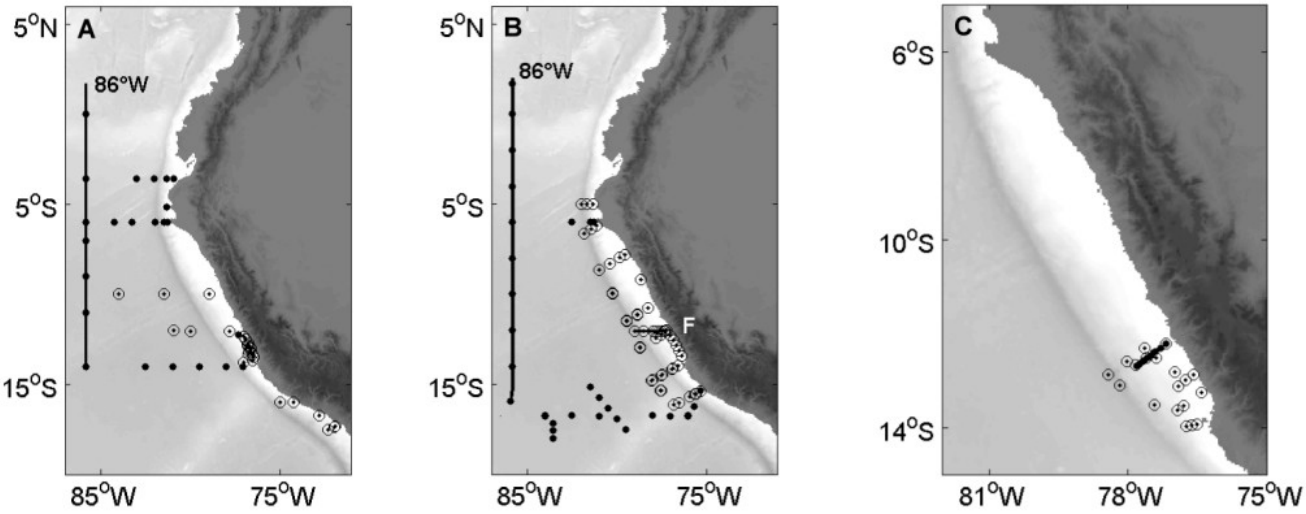

624

625

626 Figure 2:

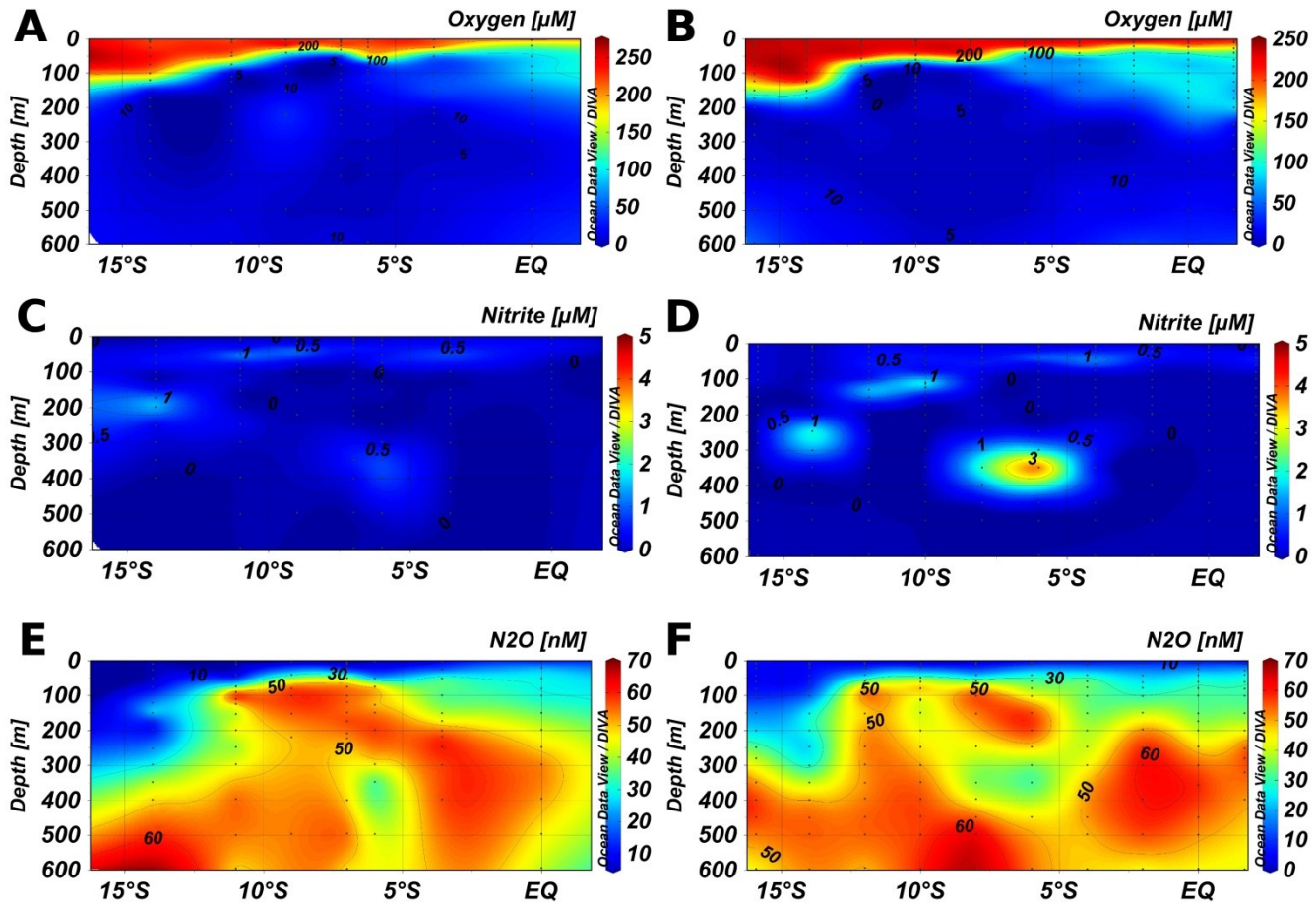

627
628

629 Figure 3:

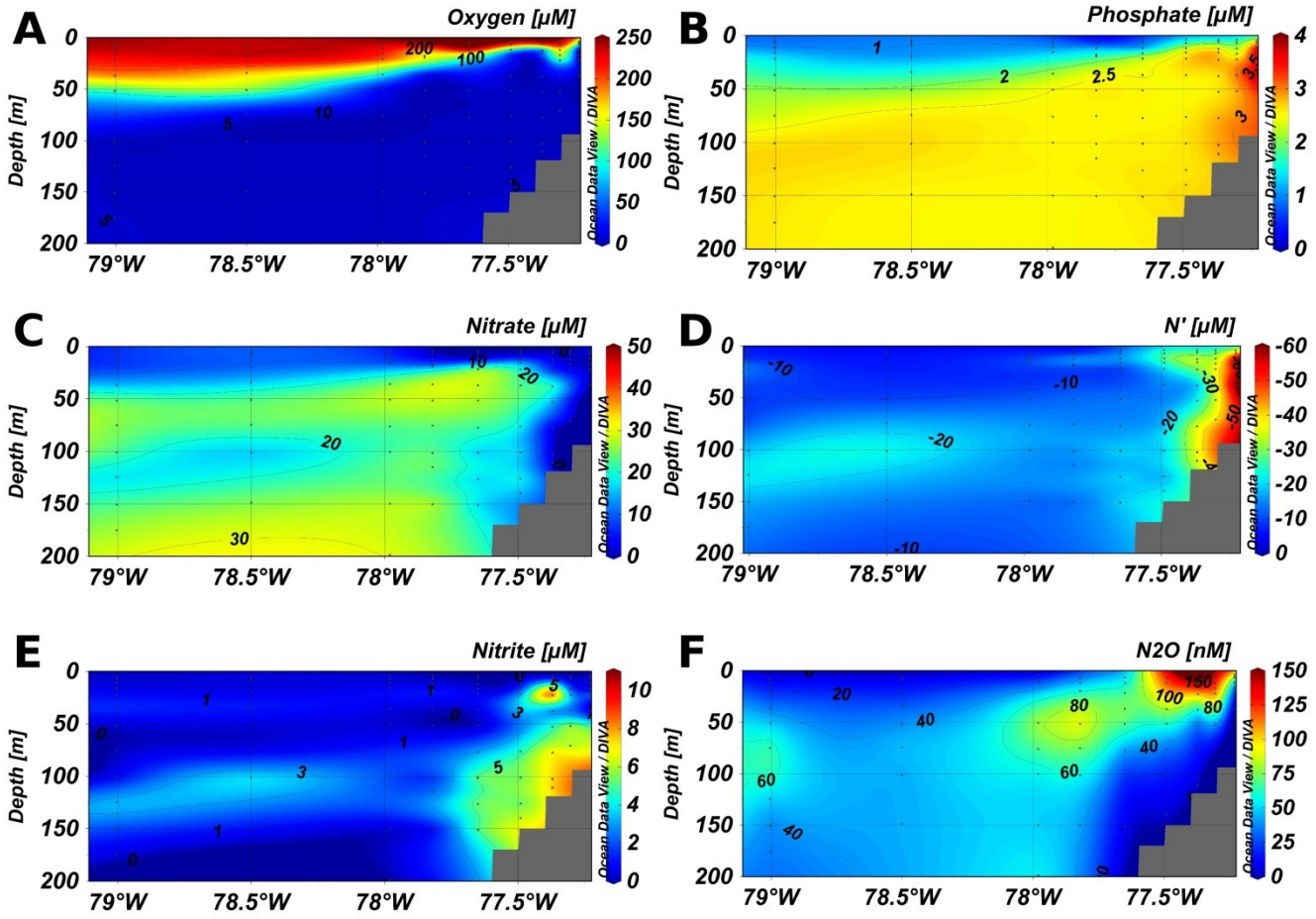

630

631

632 Figure 4:

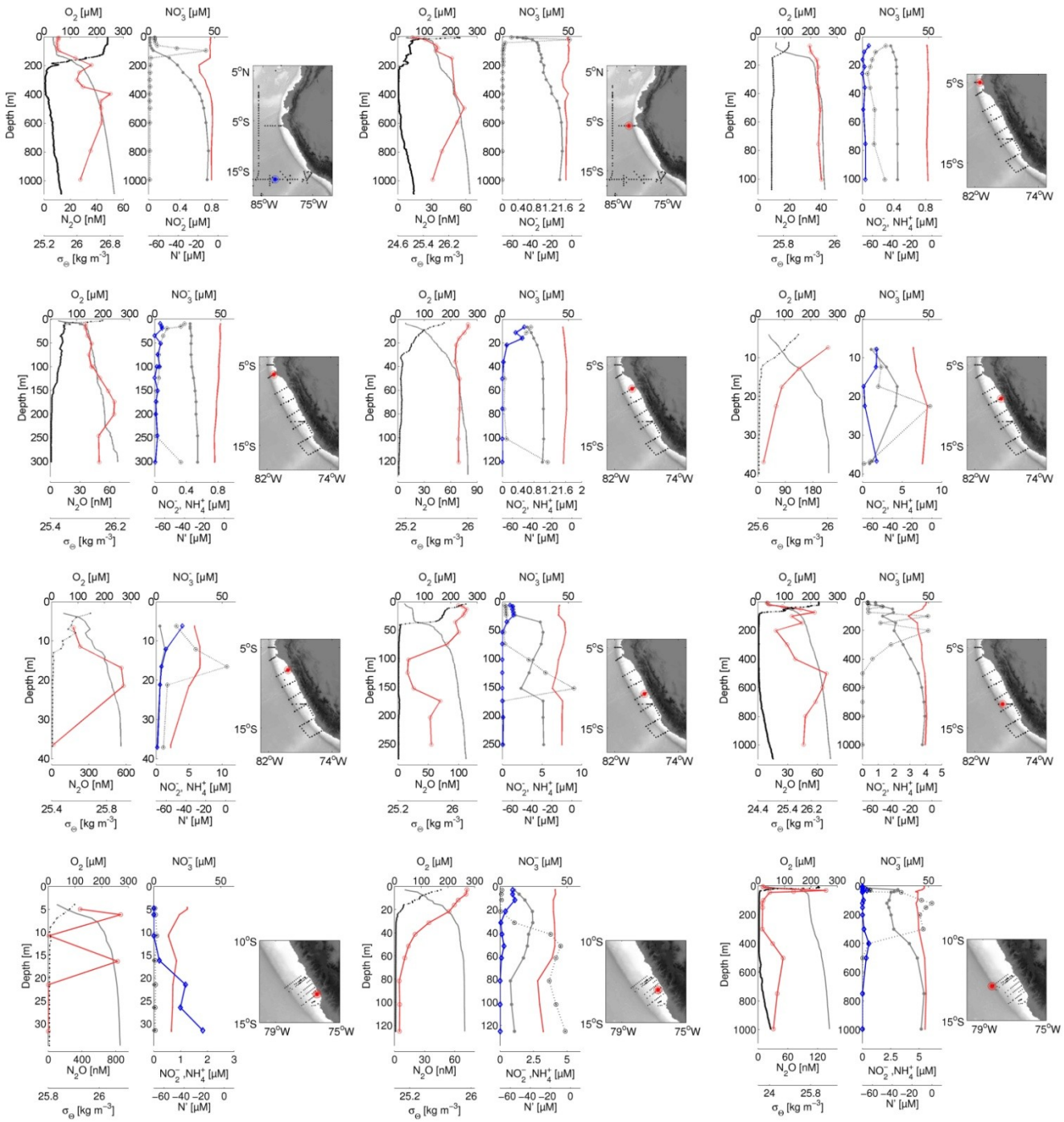

633

634

635

636 Figure 5:

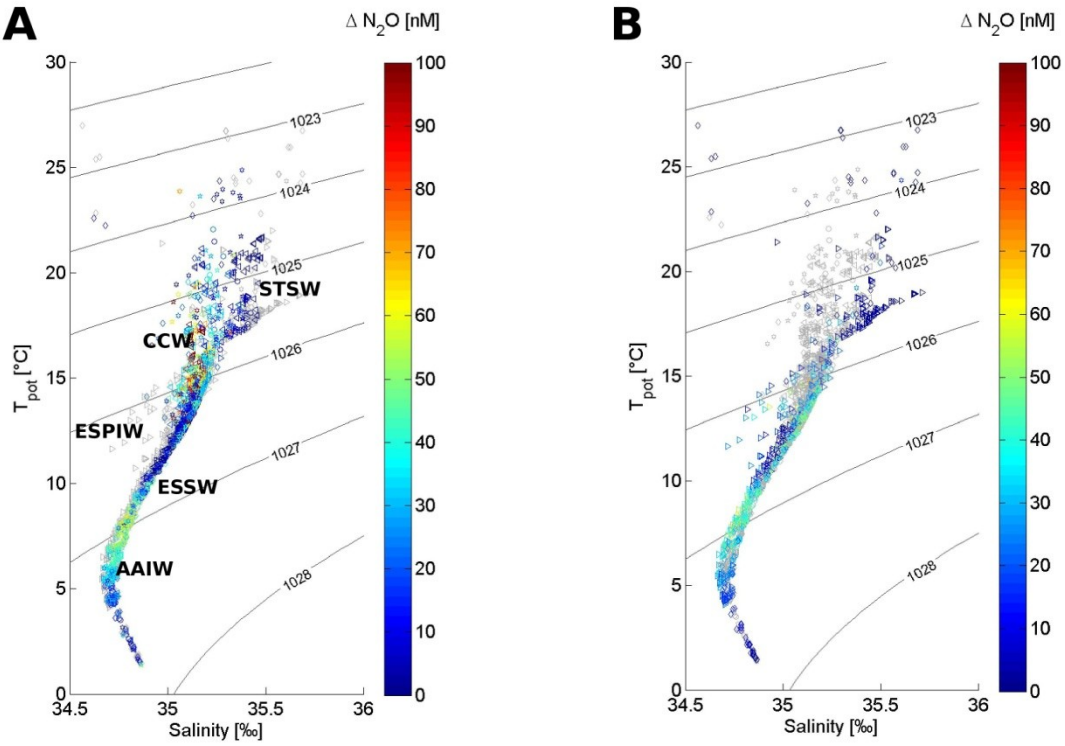

637

638 Figure 6:

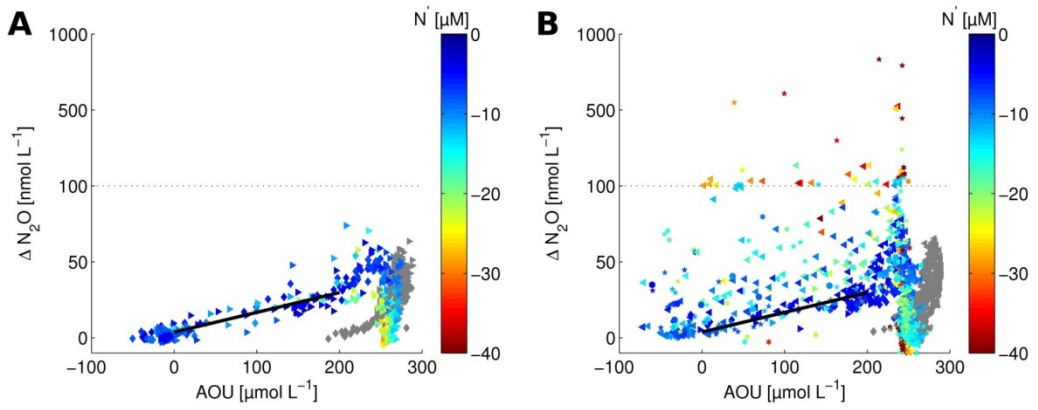

639